MSF-A Interacts with Hypoxia-Inducible Factor-1α and Augments Hypoxia-Inducible Factor Transcriptional Activation to Affect Tumorigenicity and Angiogenesis

Sharon Amir,[1] Ruoxiang Wang,[2] Haim Matzkin,[1] Jonathan W. Simons,[2] and Nicola J. Mabjeesh[1]

[1]Prostate Cancer Research Laboratory, Department of Urology, Tel Aviv Sourasky Medical Center, Tel Aviv, Israel and [2]Winship Cancer Institute, Emory University School of Medicine, Atlanta, Georgia

Abstract

Hypoxia-inducible factor-1 (HIF-1) is a key transcription factor in the signaling pathway that controls the hypoxic responses of cancer cells. Activation of the HIF system has been observed in carcinogenesis and numerous cancers. We found an interaction between a member of the mammalian septin gene family (MSF-A) and the HIF system. MSF-A is a nuclear protein that interacts with HIF-1α protein to prevent its ubiquitination and degradation, thus activating the HIF transcriptome. Cells overexpressing MSF-A protein exhibit increased HIF transcriptional activity and higher proliferation rates *in vitro* and *in vivo*. Xenograft-derived human tumors from these cells were larger and more vascular. These findings link a function of a septin protein with angiogenesis through activation of the HIF pathway. (Cancer Res 2006; 66(2): 856-66)

Introduction

Hypoxia-inducible factor 1 (HIF-1) is a key transcription factor that regulates the responses and cellular adaptation and survival to changes in oxygen tension in physiologic and pathophysiologic processes (for review, see refs. 1–6). HIF-1 is composed of the oxygen-regulated subunit, HIF-1α, and the constitutively expressed HIF-1β subunit. HIF-1α is constitutively produced and degraded under normoxic conditions. The process is triggered by posttranslational HIF-1α hydroxylation on specific proline residues (402 and 564) within the O_2-dependent degradation domain via prolyl hydroxylases in the presence of O_2, iron, and 2-oxoglutarate (7–10). The hydroxylated protein is then recognized by von Hippel Lindau protein (VHL), which is a part of an E3 ubiquitin ligase complex, ubiquitinated, and targeted to proteasomal degradation. Concurrently, hydroxylation of the asparagine residue 803 occurs by an asparaginyl hydroxylase (FIH-1), which, in turn, blocks the coactivators p300 and cyclic AMP-responsive element binding protein–binding protein (CBP) to bind to the HIF-1α subunit (11–13). Under hypoxia, HIF-1α remains unhydroxylated and does not interact with VHL, and translocates to the nucleus where it joins HIF-1β and CBP/p300 to bind hypoxia-response elements (HRE) in target genes. HIF-1 drives the transcription of over 70 genes that are important for adaptation and survival under hypoxia, including glycolytic enzymes, the glucose transporters *Glut-1* and *Glut-3, endothelin-1* (*ET-1*), *vascular endothelial growth factor* (*VEGF*), *carbonic anhydrase IX* (*CA-IX*), and *erythropoietin* (6).

The hypoxic response pathway is an important contributor to a number of common human cancers (14, 15). Increased levels of HIF-1 activity are often associated with increased tumor aggressiveness, therapeutic resistance, and mortality (6, 14). HIF-1 can be induced as a result of the high growth rate of tumor cells and intratumoral hypoxia as well as by O_2-independent genetic alterations that activate a variety of oncogenic signaling pathways or, alternatively, inactivate tumor suppressors (16). The effect of HIF-1 on tumor growth, however, is complex. Different genetic studies using embryonic stem cells or mouse embryonic fibroblasts have indicated that loss of HIF-1α or disruption of HIF-1 function causes tumor growth retardation (17–19), whereas others showed that HIF-1α acts as a tumor suppressor, or a "negative factor," in embryonic stem cell–derived tumors (20).

The mechanisms by which oncogenes or tumor suppressor genes affect the aerobic induction of HIF function in cancer cells are not completely elucidated. A better understanding of such mechanisms would not only reveal how the HIF pathway is dysregulated in cancer but also opens the way to new therapeutic approaches to target "normoxic" tumor cells (21). Here, we describe a novel association between HIF-1α protein and a myeloid/lymphoid leukemia septin-like fusion protein (MSF-A). MSF-A is a member of the septin gene family (also designated *SEPT9*_v1a) and was first identified as a part of a fusion protein with *MLL* gene in a therapy-induced acute myeloid leukemia patient (22). The exact function and cellular localization of MSF-A protein have not been well defined. Recent works suggest novel functions for septins in vesicle trafficking, cytokinesis, and oncogenesis (23, 24). The altered expression of *SEPT9* and other septins in various human cancers (25, 26) and the protein-protein interaction of MSF-A with HIF-1α protein led us to hypothesize that the MSF-A/HIF-1α complex could have a role in tumorigenesis. We tested the hypothesis that MSF-A has a role in the aerobic and hypoxic regulation of HIF-1α protein stabilization and its consequent effects on tumor growth and angiogenesis. Our data suggest that MSF-A stabilizes HIF-1α protein by preventing its ubiquitination and, consequently, activates HIF downstream survival genes to promote tumor progression and angiogenesis.

Materials and Methods

Cell Lines and Reagents

Human prostate cancer PC-3 and CL-1 cells were cultured in RPMI 1640. HEK 293 cells were maintained in DMEM. All media were supplemented with 10% FCS and antibiotics. Cells were cultured at 37°C in a humidified atmosphere and 5% CO_2 in air. For hypoxic exposure, cells were placed in a

Note: Supplementary data for this article are available at Cancer Research Online (http://cancerres.aacrjournals.org/).

Requests for reprints: Nicola J. Mabjeesh, Prostate Cancer Research Laboratory, Department of Urology, Tel Aviv Sourasky Medical Center, 6 Weizmann Street, 64239 Tel Aviv, Israel. Phone: 972-52-4262863; Fax: 972-3-6973183/6973798; E-mail: nicolam@tasmc.health.gov.il.

doi:10.1158/0008-5472.CAN-05-2738

sealed modular incubator chamber (Billups-Rothenberg, Del Mar, CA) flushed with 1% O_2, 5% CO_2, and 94% N_2.

MG-132 and cycloheximide were purchased from Sigma-Aldrich Co. (St. Louis, MO).

Plasmids and Antibodies

A Flag-MSF-A construct was prepared by reverse transcription-PCR (RT-PCR) using the forward 5′-GACTAAGCTTATGAAGAAGTCTTACTCAG-GAGGCACGCGGACC-3′ and reverse 5′-ACGTTCTAGATTACTACATCTC-TGGGGCTTCTGGCTCCTTCTCCTCC-3′ PCR primers designed according to MSF-A cDNA sequence (Genbank accession no. AF189713). MSF-A cDNA was subcloned into the p3XFLAG-myc-CMV-25 (Sigma-Aldrich) at *Hin*dIII/*Xba*I sites to provide the Flag tag at the NH_2 terminus. The NH_2-terminal truncated form of MSF-A (ΔN; deletion of the first 25 amino acids) was constructed by using the forward 5′-GACAAGCTTGCCTTGAAAAGATC-TTTTGAGGTC-3′ and the aforementioned reverse primers. The product was subcloned into the p3XFLAG-myc-CMV-25 at the *Hin*dIII/*Xba*I sites. An MSF-A mutant lacking the GTP-binding domain (ΔG; deletion of amino acids 305-312, GQSGLGKS) was generated by two PCR reactions. In the first reaction, we used the forward primer corresponding to the NH_2-terminal and an internal reverse 5′-TGGATTTGAAGAGGGTGTTGATTAAGGTGACCAC-CATGATGTTGAACTCGAAGCCC-3′ primer lacking 24 nucleotides corresponding to the GTP-binding sequence. In the second reaction, we used the antisense of the internal primer as a forward primer and the reverse primer corresponding to the COOH terminus. The overlapping two PCR products were used as a template to obtain the full length of the ΔG mutant of MSF-A. The product was subcloned into the p3XFlag-myc-CMV-25 vector. HIF-1α cDNA (Genbank accession no. NM_001530) was subcloned at *Not*I/*Xba*I sites of the p3XFLAG-myc-CMV-25 vector to provide Flag-tagged HIF-1α at its NH_2 terminus using the following PCR primers: forward 5′-ACGTGCGGCCGCGATGGAGGGCGCCGGCGGCGCGAACG-3′ and reverse 5′-CAGTTCTAGATTATCAGTTAACTTGATCCAAAGCTCTG-AG-3′. HIF-1α cDNA was cut and pasted at the *Not*I/*Xba*I sites of pcDNA3.1(+) expression vector (Invitrogen Life Technologies, Carlsbad, CA) to obtain the untagged HIF-1α wild-type. All constructs were verified by DNA sequencing (Danyel Biotech, Rehovot, Israel).

The following primary antibodies were used: mouse monoclonal anti-HIF-1α (BD Biosciences, San Diego, CA), mouse monoclonal anti-HIF-1β (Novus Biologicals, Littleton, CO), goat polyclonal antiactin, mouse monoclonal antiubiquitin (Santa Cruz Biotechnology, Inc., Santa Cruz, CA), mouse monoclonal, anti-α-tubulin and anti-Flag (Sigma-Aldrich), mouse monoclonal anti-CD-34 and anti-Ki67 (DakoCytomation, Glostrup, Denmark). Secondary antibodies for Western blotting were horseradish peroxidase conjugated (Jackson ImmunoResearch, West Grove, PA). Secondary antibodies for immunofluorescence staining were Alexa Fluor 488 goat anti-mouse and Rhodamine Red-X goat anti-rabbit (Molecular Probes, Eugene, OR).

Protein Extraction, Immunoprecipitation Assays, and Immunoblot Analysis

Whole cell extract or fractionation to nuclear and cytosolic extract were prepared as previously described (27). Protein concentration was determined using a bicinchoninic acid protein assay kit (Pierce, Rockford, IL). For immunoprecipitation, cells grown in 10 cm plates were washed with ice-cold PBS and processed as described (27, 28). Proteins were analyzed by immunoblotting with antibodies as displayed in the figures as described (27, 28).

Protein Sequencing

Whole cell extract from PC-3 cells growing under normoxia were subjected to immunoprecipitation with HIF-1α antibodies. The immunoprecipitates were analyzed on SDS-PAGE. The gel was then stained with Coomassie blue. The broad 70 kDa band species were extracted and digested overnight at 37°C. The peptides were extracted, desalted (40%) with c18ziptip, and analyzed by matrix assisted laser desorption/ionization-time of flight-mass spectrometry (Microchemical Facility, Winship Cancer Institute, Emory University School of Medicine, Atlanta, GA). The monoisotopic peptides were then searched in the NCInr database using PROWL.

Transient Transfection

Cells were seeded at 50% to 70% confluence in 10 cm or six-well plates and were transfected with a total of 1 μg DNA per well of six-well plates or 5 μg DNA/10 cm plates using GenePorter transfection reagent (Gene Therapy Systems, Inc., San Diego, CA) as previously described (27, 28).

Stable Transfection

PC-3 cell were seeded at 50% confluence in 100-mm-diameter dishes and grown overnight in complete medium. Transfections were carried out with p3XFlag-CMV-myc-25, which expresses a neomycin resistance gene. Cells were transiently transfected with either the empty vector or the vector carrying MSF-A as described above. After 48 hours, the medium was replaced with fresh medium supplemented with 1 g/mL neomycin (G418; Sigma-Aldrich) and was changed every 3 days. Two to 3 weeks later, neomycin-resistant colonies were isolated and grown in medium supplemented with 500 mg/mL neomycin. Cells were also screened for Flag-MSF-A expression by Western blotting. To avoid clonal variation of the stably transfected cells, we pooled 30 neomycin-resistant clones of PC-3 stably transfected with the empty vector (designated as PC-3-Neo) and also pooled 30 resistant clones stably transfected with MSF-A (designated as PC-3-MSF-A).

Reporter Gene Assay and Luminescence Measurements

HRE-dependent luciferase activity was done using the pBI-GL construct (pBI-GL V6L) containing six tandem copies of the *VEGF* HRE as previously described (27, 29).

Isolation and Analysis of RNA

Total RNA was extracted from cells using RNeasy Mini kit (Qiagen, Inc., Valencia, CA) and from xenograft-derived tumors was prepared using TRI Reagent (Sigma-Aldrich) following the instructions of the manufacturer. One microgram of total RNA was reverse transcribed into cDNA using Reverse-iT 1st Strand Synthesis kit (ABgene, Epsom, United Kingdom) using anchored oligo(dT) as first-strand primer. PCR was done in 25 μL reaction mixture using ReddyMix PCR master mix (ABgene). Semiquantitative RT-PCR was done using β-actin as an internal control to normalize gene expression for the PCR templates. The PCR cycle number was optimized for each primer set. Sequences of the PCR primers, number of cycles, annealing temperature, and product size for each gene are presented in Supplementary Table S1.

HIF-1α Protein Stability Assays

Cells were plated into six-well plates and grown to 70% confluence. The cells were subjected either to cycloheximide treatment or to metabolic labeling and pulse chase assay as previously described (28).

Tumor Models and Immunohistochemistry

PC-3-Neo or PC-3-MSF-A cells (3×10^6) were injected s.c. into the right hinds of CD1/nude mice. All procedures were done in compliance with the Tel Aviv Sourasky Medical Center Animal Care and Use Committee and NIH guidelines. The animals were monitored for tumor development twice a week. Tumor variables were measured with calipers and tumor volume was calculated according to the following formula: tumor volume = width^2 × length × 0.52. After 6 weeks, the animals were sacrificed and tumors were excised as quickly as possible, weighed and cut into two pieces. One piece of tumor was fixed with 4% buffered formalin for 24 hours and embedded in Paraplast (Oxford Labware, St. Louis, MO) until immunohistochemical staining, and the rest of the tumor was immediately frozen in liquid N_2 and kept at −80°C for RNA analysis.

For immunohistochemical staining, paraffin-embedded tissue was sectioned into 3 μm thickness and mounted on Superfrost/plus slides (Menzel-Gläser, Braunschweig, Germany). The sections were processed for immunostaining with anti-CD34 (1:50 dilution) or anti-Ki67 (1: 25 dilution) for 30 minutes at room temperature as previously described (30). For negative controls, the exact procedure was done with either the omission of the primary or the secondary antibody. Positive staining cells and microvessels were counted for quantitative analysis of Ki67 and CD34 staining, and their density was expressed as the number of positive cells per total number of cells or capillaries per total section area excluding necrotic areas, respectively.

Production of Sequence-Directed Antibodies against MSF-A Protein

A peptide of 15 amino acids corresponding to the NH_2-terminal part of MSF-A protein (amino acids 3-17; KSYSGGTRTSSGRLR) was synthesized, conjugated to a carrier protein, and injected into rabbits (Convance Research Products, Inc., Denver, PA). The sequence of the peptide was selected from the unique region of MSF-A. The sera drawn from the rabbits were tested for MSF-A immunoreactivity using immunoprecipitation and Western blotting.

Immunofluorescence and Confocal Microscopy

Exponentially growing cells were plated on 12-mm glass coverslips (Fisher Scientific, Pittsburgh, PA) into 24-well plates and allowed to attach overnight. On the following day, the cells were subjected to hypoxia for 16 hours after which they were fixed with PHEMO buffer [PIPES 0.068 mol/L, HEPES 0.025 mol/L, EGTA 0.015 mol/L, $MgCl_2$ 0.003 mol/L, 10% DMSO (pH 6.8)] containing 3.7% formaldehyde, 0.05% glutaraldehyde, and 0.5% Triton X-100 for 10 minutes at room temperature. Coverslips were processed for double-labeling immunofluorescence with monoclonal mouse anti-HIF-1α and polyclonal rabbit anti-MSF-A antibodies as described (28).

In Vitro Proliferation Assays

Cell proliferation assay with 2,3-bis[2-methoxy-4-nitro-5-sulfophenyl]-2*H*-tetrazolium-5-carboxanilide reagent. PC-3-Neo and PC-3-MSF-A cells were seeded in 96-well plates (1,000 per well in 200 μL). On the next day, the cells were cultured either under normoxic or hypoxic conditions. After the indicated time, cell proliferation was measured using a 3-bis-(2-methoxy-4-nitro-5 sulfenyl)-(2*H*)-tetrazolium-5-carboxanilide (XTT) kit (Biological Industries Ltd., Kibbutz Beit Haemek, Israel) following the instructions of the manufacturer.

Plating efficiency assay. PC-3-Neo and PC-3-MSF-A cells were cultured in 100-mm-diameter plates (1,000 per plate) and incubated to allow colony formation. The cultures were monitored on a daily basis and, when colonies were visible (after ~2 weeks), the cells were fixed and stained with 90% ethanol, 5% acetic acid, 0.01% Coomassie brilliant blue (Sigma-Aldrich). Plating was done in triplicate, and colonies containing ≥20 cells were counted. Plating efficiency (%) was calculated as the number of colonies formed / number of cells plated × 100.

Soft agar foci assay. This assay tests the anchorage-independent growth of the cell in soft agar. Suspensions of PC-3-Neo or PC-3-MSF-A cells in 0.22% soft agar were poured on 35-mm-diameter plates (5,000 per plate) precast with 0.5% soft agar and the cells were cultured for 4 weeks. Colonies (≥20 cells) were counted.

Tumor Array and Dot Blot Analysis

An MSF-A cDNA (*Hin*dIII/*Eco*RI) was labeled with [α^{32}P]dCTP (Qiagen) and used to probe the Human Matched Tumor/Normal Expression Array from Clontech (Mountain View, CA) under high stringency conditions following the instructions of the manufacturer. Washed filters were exposed to autoradiographic films. The membrane was stripped and reprobed with a labeled β-actin probe for normalization. Dots densities were analyzed using densitometry and each MSF-A dot was normalized to its corresponding β-actin dot. The ratio between tumoral and normal expression of each pair was then calculated.

Data Analysis

Experiments presented in the figures are representative of three or more different repetitions. Quantification of band densities was done using the public domain NIH Image (version 1.61). Statistical analysis was done using a one-way ANOVA test, and $P < 0.05$ was considered statistically significant.

Results

MSF-A interacts with HIF-1α protein and increases HIF-1 transcriptional activity. Because the human prostate cancer PC-3 cells express substantial amounts of HIF-1α protein even under normoxic conditions (31), they were used to identify new candidates interacting with HIF-1α protein. PC-3 cells were grown under normoxic conditions and metabolically labeled with [^{35}S]methionine. Whole cell lysates were then subjected to coimmunoprecipitation experiments using monoclonal antibody to HIF-1α. Under these coimmunoprecipitation conditions (see Materials and Methods), an intense 70 kDa band (Fig. 1*A*) was observed, and we identified the protein as MSF-A by using amino acid sequence analysis (data not shown). Neither the localization nor the function of MSF-A protein, as is the case for many other septin members, have been clarified thus far. To confirm the interaction between HIF-1α and MSF-A proteins, we subcloned the cDNA encoding the wild-type MSF-A into an expression vector containing Flag tag in the NH_2-terminal side. Transient transfection of MSF-A plasmid into HEK 293 cells resulted in a time-dependent expression of a 70 kDa Flag-tagged protein that corresponded to the predicted MSF-A protein (Supplementary Fig. S1). We next transiently cotransfected HEK 293 cells with expression vectors encoding Flag-MSF-A and untagged HIF-1α. Whole cell lysates were prepared under normoxic conditions and subjected to coimmunoprecipitation studies using antibodies to Flag or HIF-1α. The immunoprecipitated proteins from each lysate were analyzed by Western blotting with each counterpart antibody (Fig. 1*B*). HIF-1α antibody immunoprecipitated Flag-MSF-A protein whereas Flag antibody immunoprecipitated HIF-1α protein in cells transfected with HIF-1α and Flag-MSF-A (Fig. 1*B*). On the other hand, under these normoxic conditions, Flag antibody failed to coimmunoprecipitate HIF-1β protein (Fig. 1*B*), whereas HIF-1α antibody pulled down HIF-1β mainly under hypoxic conditions (data not shown).

We also studied the effects of MSF-A on HIF-1 transcriptional activity using a reporter gene assay as previously described (27, 29). PC-3 cells were transiently cotransfected with a reporter plasmid containing the *luciferase* gene under the control of HRE from the *VEGF* promoter and with the empty vector control or the MSF-A expression vector. The cells were subsequently grown under normoxia or exposed to hypoxia. In control cells (transfected with empty vector), hypoxia induced luciferase activity by >15-fold compared with normoxia, whereas the hypoxic induction of luciferase activity was up to 50-fold in cells transfected with MSF-A (Fig. 1*C*). Similar results were also obtained in HEK 293 cells (data not shown). These findings confirmed a new protein of the septin family interacts with HIF-1α protein and augments HIF transcriptional activity.

The activation of HIF-1 by MSF-A is dependent on the intact NH_2-terminal and GTP-binding domains of MSF-A protein. Members of the evolutionarily conserved septin family of genes have a well-conserved GTP-binding domain and possess GTPase activity. *SEPT9* has been shown to have a complex genomic architecture, such that up to 15 different isoforms are possible by the shuffling of five alternate NH_2 termini and three alternate COOH termini. The first 25 amino acids of the MSF-A protein are uniquely different from any other member of the overall septin family. Therefore, we decided to test the effects of the most variable and conserved domains of MSF-A on HIF. Using deletion mutagenesis methods, we designed an MSF-A mutant lacking the first 25 amino acids (ΔN) and another lacking the GTP-binding domain (ΔG). Expression of escalating amounts of the ΔN mutant of MSF-A induced a dose-dependent inhibition of HIF-1 transcriptional activity, whereas the expression of wild-type MSF-A induced HIF activity (Fig. 1*D*). In contrast, the expression of the ΔG mutant of MSF-A had no effect on HIF activity (Fig. 1*E*). Interestingly, immunoprecipitation experiments showed that both ΔN and ΔG

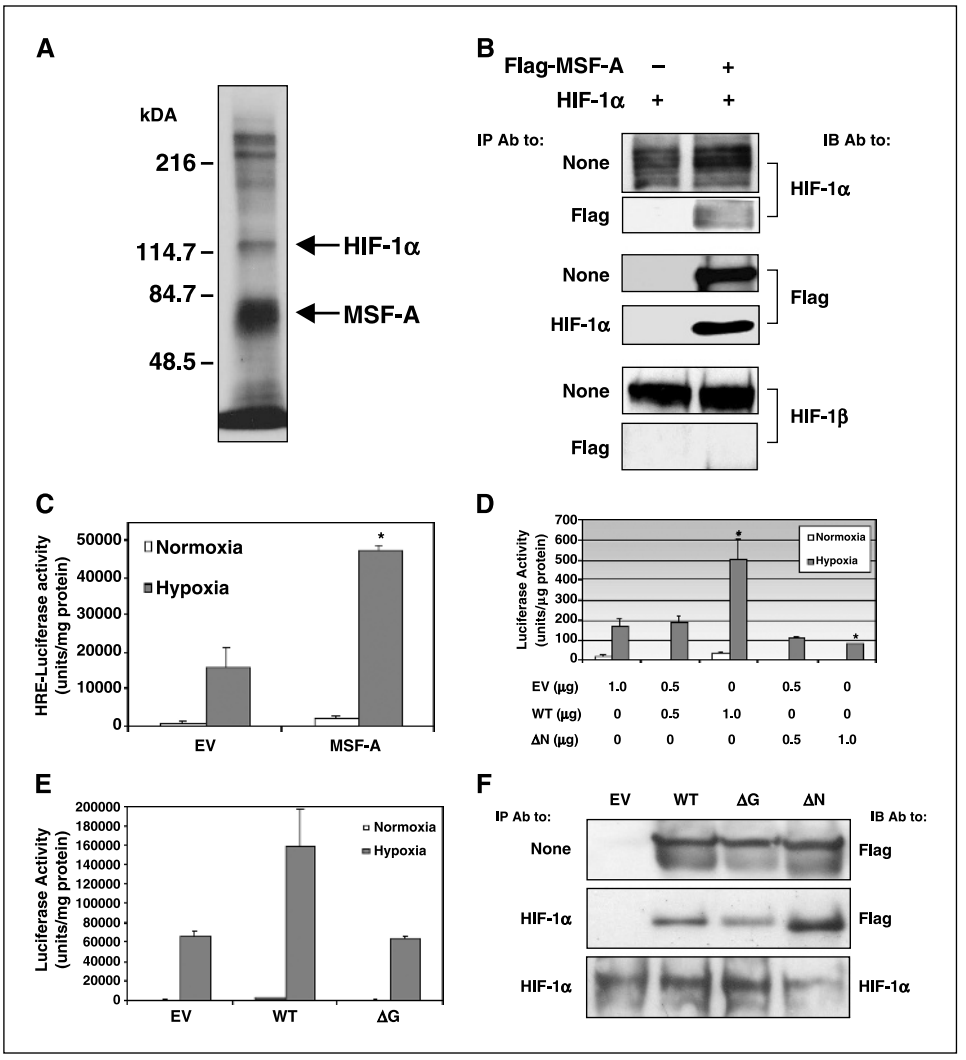

Figure 1. MSF-A interacts with HIF-1α protein and up-regulates HIF-1 transcriptional activity. *A,* PC-3 cells were labeled with [^{35}S]methionine, subjected to immunoprecipitation with HIF-1α antibody, analyzed on SDS-PAGE, and visualized by autoradiography. *B,* HEK 293 cells were transiently cotransfected with expression vector encoding untagged HIF-1α, Flag-MSF-A, or empty vector. The cells were lysed, subjected to immunoprecipitation (*IP*) using HIF-1α or Flag antibodies (*Ab*) and then immunoblotted (*IB*) with HIF-1α, Flag, or HIF-1β antibodies. *None,* no immunoprecipitation, whole cell extract samples. *C,* PC-3 cells were cotransfected with a pBI-GL V6L expressing luciferase under the control of HRE and with expression vector encoding MSF-A or empty vector. After 24 hours of transfection, the cells were subjected overnight to normoxia or hypoxia and then analyzed for luciferase luminescence assay. Relative luciferase activity, units/mg protein at each assay point. *Columns*, mean (n = 3); *bars*, SD. *, $P < 0.05$ compared with hypoxia of empty vector. *D,* HEK 293 cells were cotransfected with HRE-dependent luciferase reporter (0.1 μg) and the indicated amount (in μg; total of 1 μg) of expression vector encoding wild-type MSF-A (*WT*), NH_2-terminal truncated form of MSF-A (*ΔN*), and empty vector (*EV*). After 24 hours of transfection, the cells were subjected overnight to normoxia or hypoxia and then analyzed for luciferase luminescence assay. Relative luciferase activity, units/μg protein at each assay point. *Columns*, mean (n = 3); *bars*, SD. *, $P < 0.05$, compared with hypoxia of empty vector. *E,* HEK 293 cells were cotransfected with HRE-dependent luciferase reporter and the expression vector encoding wild-type MSF-A, the deleted GTP-binding site form of MSF-A (*ΔG*), or empty vector and were then exposed to hypoxia as described in (*A*). Relative luciferase activity, units/mg protein in each assay point. *Columns*, mean (n = 3); *bars*, SD. *F,* HEK 293 cells were transiently cotransfected with expression vector encoding Flag-MSF-A, Flag-ΔG, Flag-ΔN, or empty vector. After 48 hours, the cells were lysed, subjected to immunoprecipitation using HIF-1α antibody, and then immunoblotted with HIF-1α or Flag antibodies.

protein products continued to bind to HIF-1α protein (Fig. 1*F*). These results indicate that the activation of HIF-1 by MSF-A requires both the GTP-binding site and the intact NH_2 terminus of MSF-A, whereas the exact involvement of these domains in HIF activation has to be elucidated.

MSF-A increases the expression of HIF downstream genes. To further study the role of MSF-A in cancer cells, we stably transfected PC-3 cells with MSF-A and studied their characteristics on HIF. Neomycin-resistant PC-3 cells were selected and screened for the expression of Flag-MSF-A using Western blotting (Fig. 2*A*). Clones with different MSF-A expression levels were tested for HIF-1 transcriptional activity using an HRE reporter gene assay. There was a corresponding increase of HIF-1 transcriptional activity with MSF-A protein levels (Fig. 2*A*). As an internal control, cells were cotransfected with both *Renilla* SV40-luciferase and the firefly HRE-luciferase and subjected to dual luciferase assay. There were no changes in *Renilla* SV40-luciferase activity under hypoxia or between the different clones compared with empty vector control or parental PC-3 cells (data not shown). To avoid biases from clonal variations of MSF-A overexpressing cells, we pooled 30 neomycin-resistant clones of stably transfected cells with empty vector control (PC-3-Neo) and cells stably transfected with MSF-A (PC-3-MSF-A). We next tested the pooled cells for HIF-1 transcriptional activity. Again, PC-3-MSF-A cells still exhibited a significant

increase (2.5-fold, $P < 0.01$) of HIF-1 transcriptional activity compared with PC-3-Neo cells (data not shown). To further show the effects of MSF-A on HIF-target genes, we used a semiquantitative RT-PCR and quantitative real-time PCR analyses. Total RNA was prepared from both PC-3-Neo and PC-3-MSF-A cells and was reverse transcribed. PCR analysis showed that the mRNA levels of the angiogenic factor VEGF were significantly higher in the PC-3-MSF-A cells than in the PC-3-Neo cells, whereas HIF-1α mRNA levels were not changed (Fig. 2*B*). Other HIF-target genes, including *Glut-1, CA-IX*, and *ET-1*, were also up-regulated to varying extent in PC-3-MSF-A cells (Fig. 2*B*). Similar results were also obtained using quantitative real-time PCR analysis (Supplementary Fig. S2). These data further showed that the introduction of MSF-A enhances HIF-1 transcriptional activity.

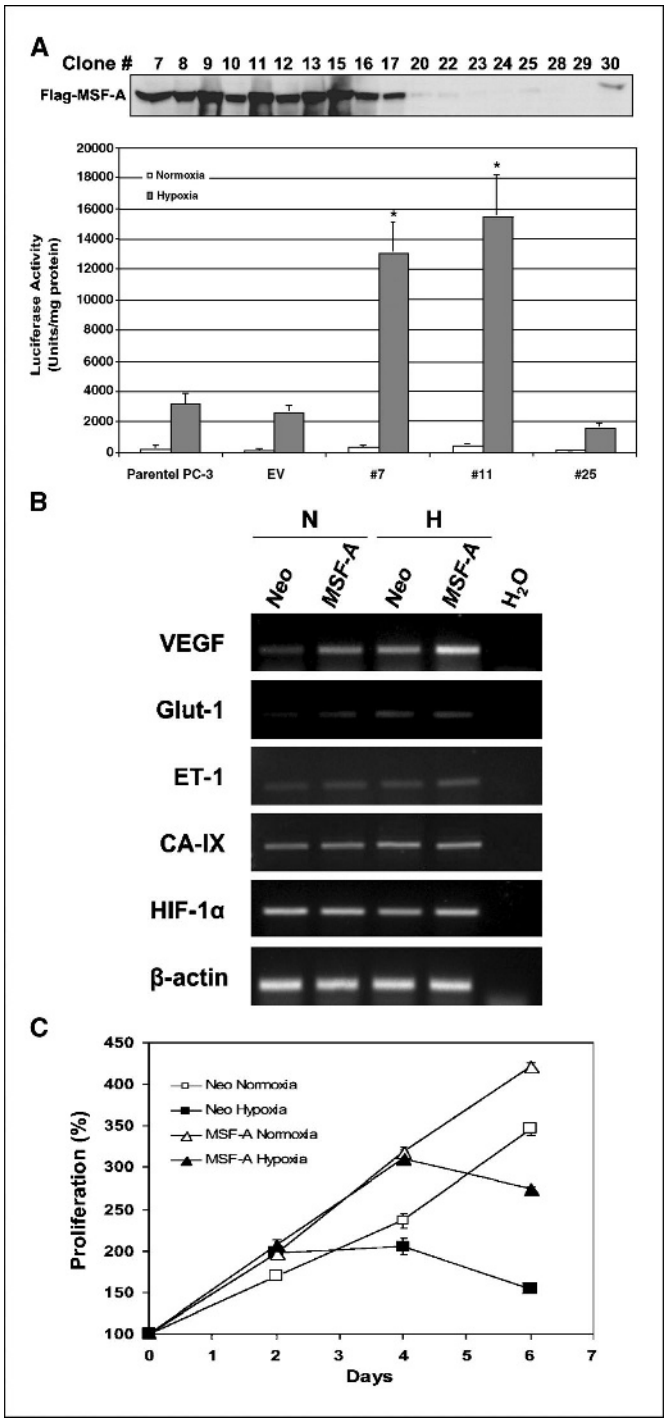

Figure 2. Stable overexpression of MSF-A in PC-3 cells enhances proliferation and up-regulates HIF-1 target genes *in vitro*. *A,* PC-3 cells were stably transfected with expression vector encoding Flag-MSF-A or empty vector. Neomycin-resistant clones were grown under normoxic conditions, harvested, and analyzed for MSF-A expression by immunoblotting with Flag antibody (*top*). Parental PC-3 cells and selected stably transfected clones were transiently transfected with HRE-dependent luciferase reporter (1 μg) for HIF-1 transcriptional activity. Relative luciferase activity, units/mg protein in each assay point. *Columns*, mean ($n = 3$); *bars*, SD. *, $P < 0.05$, compared with hypoxia of empty vector (*bottom*). *B,* total RNA was isolated from PC-3-Neo and PC-3-MSF-A cells grown under normoxic and hypoxic conditions. Semiquantitative RT-PCR analysis was done using VEGF, Glut-1, ET-1, CA-IX, HIF-1α, and β-actin primers. *C,* PC-3-Neo and PC-3-MSF-A cells were grown under normoxic and hypoxic conditions for the indicated time and were then analyzed for proliferation using XTT assay. Proliferation was expressed as increase in percentage of the initial absorbance that was measured on the next day of seeding (100%). Growth media were not changed until the end of the experiment.

MSF-A expression promotes proliferation, tumor growth, and angiogenesis. Our hypothesis is that enhancing HIF-1 transcriptional activity by MSF-A would influence directly or indirectly the fate biology of cancer cells. We therefore examined the effects of MSF-A expression on cell proliferation. Using an XTT assay, we showed that the proliferation rate of PC-3-MSF-A cells is higher to a greater extent than the proliferation rate of PC-3-Neo cells under both conditions of normoxia and hypoxia (Fig. 2*C*). In addition, PC-3-MSF-A cells formed significantly larger and increased numbers of colonies compared with PC-3-Neo cells grown in soft agar (i.e., 21.7 ± 3.8 versus 9 ± 4.4 foci per plate, respectively; $n = 3$; $P < 0.05$; Supplementary Fig. S3). This was further confirmed by using the plating efficiency assay (see Materials and Methods). Again, PC-3-MSF-A cells showed higher plating efficiency compared with PC-3-Neo cells (i.e., 49.7 ± 3.7% versus 17.3 ± 3.5%, respectively; $n = 3$; $P < 0.001$; data not shown).

We next studied the effects of MSF-A on proliferation, tumor growth, and angiogenesis *in vivo*. We used a s.c. xenograft mouse tumor model to examine the growth of tumors derived from PC-3-MSF-A and PC-3-Neo cells. In this xenograft model, tumors derived from PC-3-MSF-A cells appeared earlier and exhibited increased mean volume (~2-fold) compared with tumors derived from PC-3-Neo cells (Fig. 3*A*). Although the difference in tumor volume was not statistically significant, the mean weight of PC-3-MSF-A tumors was significantly heavier than the control tumors (1.74 ± 0.4 versus 0.72 ± 0.07 g, respectively; $P < 0.05$; Fig. 3*B*). Most importantly, the phenotype of the tumors was strikingly different. Macroscopic and histologic examination showed that PC-3-MSF-A tumors were more pleomorphic, aggressive, and invasive, and that there were only scattered small areas of necrosis, whereas a large area of central necrosis was observed in the PC-3-Neo cell–derived xenografts (not shown). In addition, MSF-A overexpression significantly increased intratumoral cell proliferation and vascular density as quantified from the Ki67 and CD34 immunostaining, respectively (Fig. 3*C*). RT-PCR analysis of RNA derived from the tumors showed that the expression level of selected HIF-target genes, including *VEGF* and *CA-IX*, were elevated in PC-3-MSF-A tumors compared with PC-3-Neo tumors (Fig. 3*D*). As a control, we confirmed that PC-3-MSF-A tumor cells still expressed higher levels of MSF-A mRNA (Fig. 3*D*). Collectively, the *in vitro* and *in vivo* data indicate that MSF-A affects HIF-1 transcriptional activation, cell proliferation, and tumor angiogenesis.

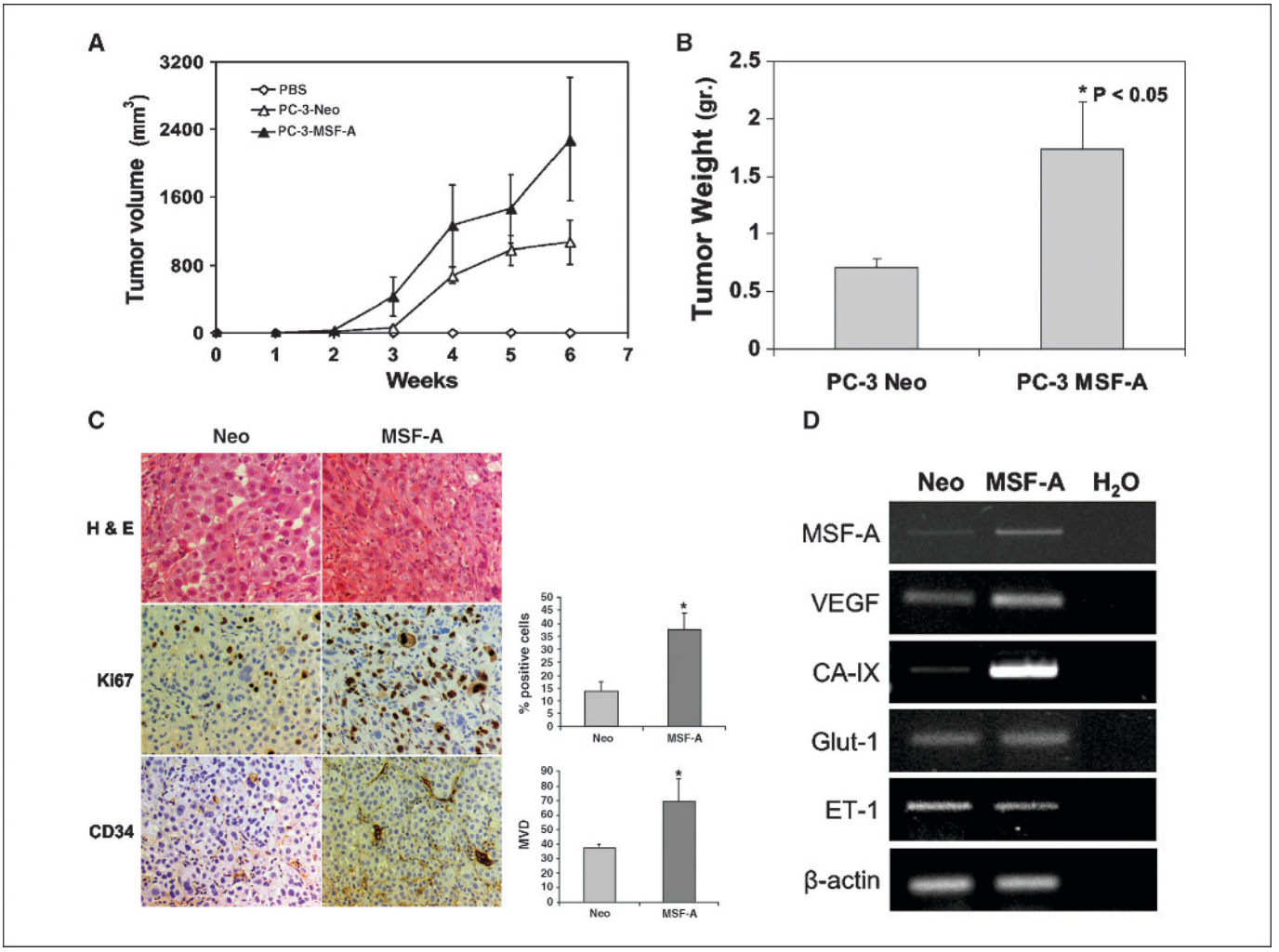

Figure 3. MSF-A expression promotes tumor growth and angiogenesis in a prostate cancer xenograft model. A prostate cancer xenograft model was established using PC-3-Neo and PC-3-MSF-A cells (3×10^6) implanted s.c. into the right hind of nude mice. PBS was used as a negative control. Animals were monitored for tumor volume measurements (*A*), sacrificed after 6 weeks, and tumors were processed for tumor weight measurements (*B*), immunohistochemical staining (*C*), and RT-PCR analysis (*D*). *A,* tumor volume measurements were calculated using the formula width^2 × length × 0.52. *Points,* mean of representative experiments ($n = 5$); *bars,* SE. *B,* tumors were weighed immediately after dissection. *Columns*, mean ($n = 5$); *bars*, SE. *, $P < 0.05$. *C,* sections from both PC-3-Neo and PC-3-MSF-A tumors were subjected to H&E and immunostaining with Ki67 and CD34 as indicated. *Right, top,* Ki67 staining (%) was quantified by dividing the number of positive nuclei by the number of total nuclei in a ×40 magnification field multiplied by 100. Samples consisted of five paraffin-embedded tumor sections from each animal per group. *Columns*, average of the means of Ki67 staining from each animal ($n = 5$); *bars*, SE. *, $P < 0.05$. *Right, bottom,* microvessel density was determined by counting the capillaries positive for CD34 staining in ×4 magnification field per total section area (excluding necrotic areas) in five paraffin-embedded tumor sections from each animal per group. *Columns*, average of the means of microvessel density from each animal ($n = 5$); *bars*, SE. *, $P < 0.05$. *D,* a representative RT-PCR analysis of RNA isolated from either PC-3-Neo or PC-3-MSF-A tumors. The primers used were specific for the indicated mRNA.

MSF-A protein colocalizes with HIF-1α in the nucleus. To learn more on the localization of MSF-A protein, we generated polyclonal antibodies directed against the unique NH_2-terminal part in the sequence of the protein. The antibodies recognized a 70 kDa protein corresponding to MSF-A protein in PC-3 and other nonprostate cancer cell lines (data not shown). To confirm specificity of the antibodies, Flag-MSF-A was expressed in HEK 293 cells and the cells were subjected to immunoprecipitation assay using an antibody to Flag and then immunoblotted with the MSF-A antibodies (Fig. 4*A*). Flag-MSF-A was also recognized by the produced antibodies against MSF-A (Fig. 4*A*) but not by other unrelated antibodies (data not shown).

We assessed the localization of MSF-A by using both biochemical fractionation and laser scanning confocal microscopy. Nuclear and cytosolic extracts were prepared from CL-1 and PC-3 cells grown under normoxia and hypoxia and subjected to immunoblotting with HIF-1α or MSF-A antibodies. As expected, HIF-1α protein was localized and accumulated in the nucleus upon hypoxic exposure (Fig. 4*B*). MSF-A protein was also predominantly localized in the nucleus without any significant change in its levels after hypoxia (Fig. 4*B*). PC-3 cells were grown either under normoxia or hypoxia and then double labeled with antibodies against MSF-A (Fig. 4*C, red staining*) and HIF-1α (Fig. 4*C, green staining*). HIF-1α was barely detectable under normoxic conditions but it accumulated in the nucleus after exposure to hypoxia (Fig. 4*C, green staining*), whereas MSF-A was detected constitutively in the nucleus under both normoxia and hypoxia conditions (Fig. 4*C, red staining*). An overlay of the stainings showed colocalization of HIF-1α with MSF-A in the nucleus (Fig. 4*C*). Nuclear localization of MSF-A

was further confirmed by double-labeling with 4′,6-diamidino-2-phenylindole (data not shown). The results are consistent with the predicted sequence analysis of MSF-A protein, which contains a bipartite nuclear targeting sequence at amino acids 2 to 18.

To further confirm the interaction between endogenous HIF-1α and MSF-A proteins, we did immunoprecipitation experiment using HIF-1α and the produced MSF-A antibodies. PC-3 and CL-1 cells were grown under normoxia or hypoxia and subjected to immunoprecipitation with HIF-1α antibodies (Fig. 4*D*). The immunoprecipitates were analyzed by immunoblotting with MSF-A antibodies. Under normoxia, the antibodies to HIF-1α pulled down both the endogenous HIF-1α protein and the endogenous MSF-A protein (Fig. 4*D*). Under hypoxia, in spite of a larger amount of HIF-1α protein within the immunoprecipitate, its interaction with MSF-A protein was much weaker, as shown in two different cell lines (Fig. 4*D*). Taken together, by using antibodies to MSF-A, we showed that MSF-A is a nuclear protein and that it colocalizes with HIF-1α protein in the nucleus. Moreover, the results show that the endogenous HIF-1α associates with the endogenous MSF-A protein with higher affinity under normoxic conditions than under hypoxic conditions.

MSF-A stabilizes HIF-1α protein by preventing its ubiquitination. To mechanistically elucidate the mechanism by which MSF-A involves HIF-1, we examined the effects of MSF-A expression on HIF-1α protein stability. As shown in Fig. 2*B* and Supplementary Fig. S2, MSF-A overexpression did not alter significantly HIF-1α mRNA levels. Our hypothesis was that MSF-A affects HIF-1α on the posttranscriptional/posttranslational level. We first studied the hypoxic induction of HIF-1α protein at a shorter rate-limiting time rather than at times to reach steady-state levels. After 4 hours of exposure to hypoxia, the levels of HIF-1α protein expressed in PC-3-MSF-A cells were significantly higher than those obtained from PC-3-Neo cells (Fig. 5*A*). We observed that the hypoxic induction of HIF-1α in PC-3-MSF-A cells was faster than in PC-3-Neo cells (compare expression levels after 4 and 8 hours of hypoxia; Fig. 5*A*). We therefore examined MSF-A effects on HIF-1α protein stability by using the protein translation inhibitor cycloheximide (Fig. 5*B*) and a pulse-chase assay (Fig. 5*C*). New protein synthesis is inhibited in the presence of cycloheximide; thus, HIF-1α levels would predominantly reflect the degradation process of the HIF-1α protein. PC-3-Neo and PC-3-MSF-A cells were exposed to cycloheximide for various times and HIF-1α protein levels were analyzed by Western blotting. Within <20 minutes of exposure to cycloheximide, HIF-1α protein levels

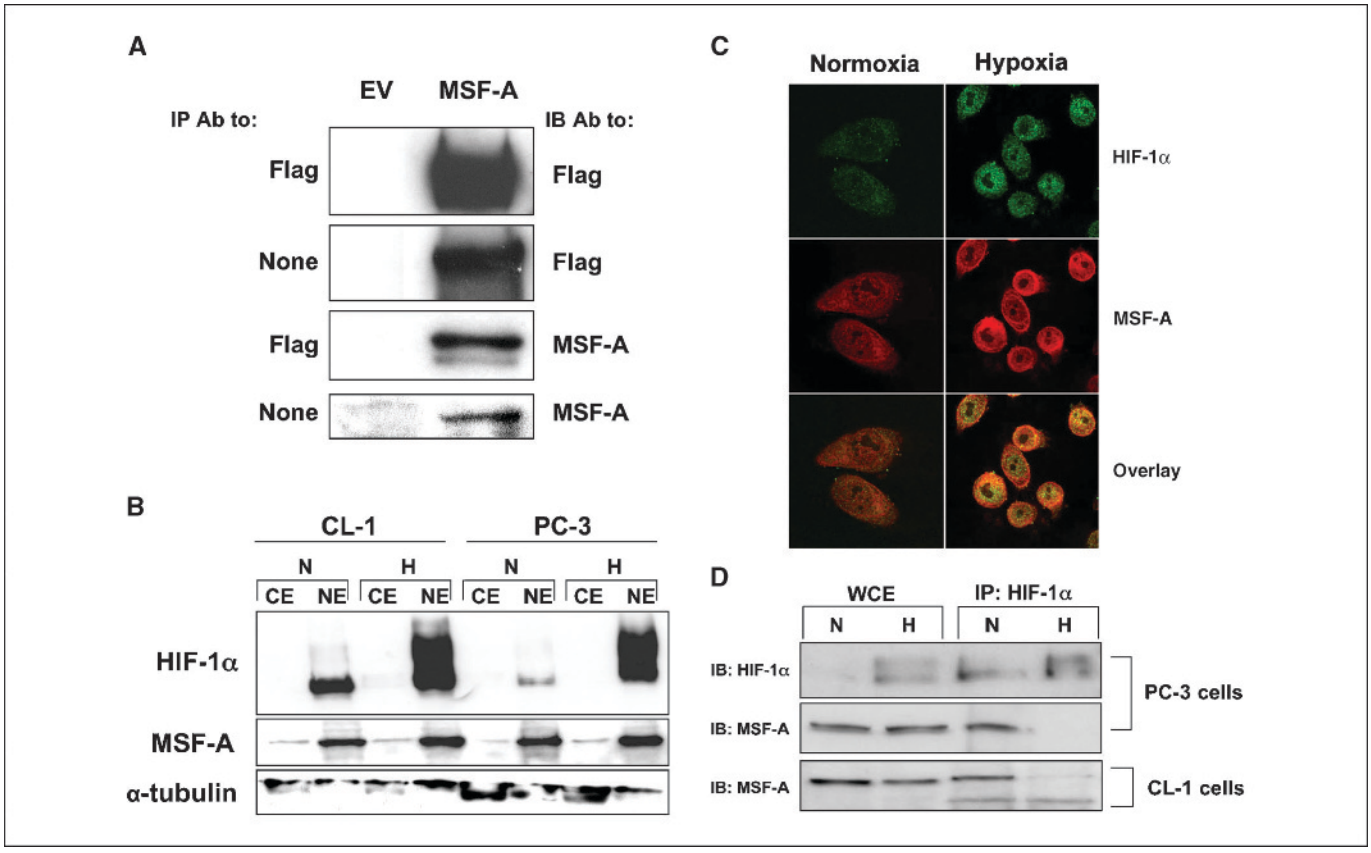

Figure 4. Cellular localization of MSF-A protein. *A,* HEK 293 were transiently transfected with expression vector encoding Flag-MSF-A or empty vector and whole cell extracts were prepared. Lysates were subjected to immunoprecipitation with Flag antibody. Immunoprecipitates were resolved on SDS-PAGE and analyzed by immunoblotting with Flag antibody or sera raised against the NH_2 terminus of MSF-A. *None,* no immunoprecipitation, whole cell extract samples. *B,* PC-3 and CL-1 cells were grown either under normoxia (*N*) or exposed to hypoxia (*H*) for 16 hours. Cytosolic (*CE*) and nuclear (*NE*) extracts were prepared, analyzed by SDS-PAGE, and immunoblotted with antibodies to HIF-1α, MSF-A, or α-tubulin. *C,* PC-3 cells were grown under normoxia or exposed to hypoxia for 16 hours and then fixed and processed for double immunofluorescence labeling with anti HIF-1α (*green staining*) and anti-MSF-A (*red staining*) antibodies. Staining was analyzed by confocal laser-scanning microscopy. *D,* PC-3 and CL-1 cells were grown under normoxia or hypoxia for 16 hours. Whole cell extracts (*WCE*) were subjected to immunoprecipitation with HIF-1α antibody. Immunoprecipitates were analyzed on SDS-PAGE and immunoblotted with HIF-1α or MSF-A antibodies.

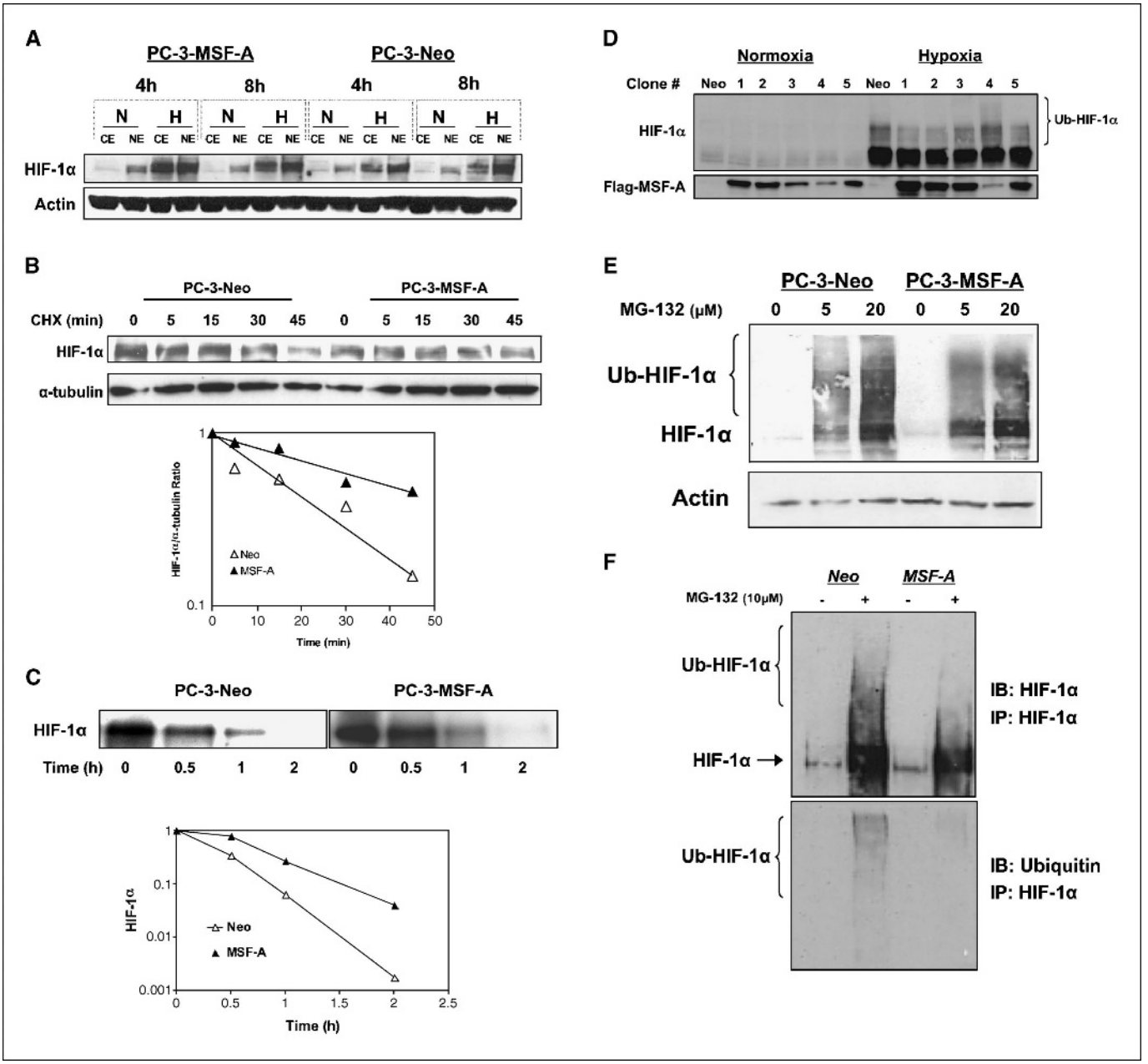

Figure 5. MSF-A stabilizes HIF-1α protein and reduces its ubiquitination. *A,* PC-3-Neo and PC-3-MSF-A cells were grown under normoxia or subjected to hypoxia for the indicated time. Cytosolic (*CE*) and nuclear (*NE*) extracts were prepared, analyzed by SDS-PAGE, and immunoblotted with antibodies to HIF-1α and actin. *B,* PC-3-Neo and PC-3-MSF-A cells were grown under normoxia, and cycloheximide was then added at a final concentration of 10 μg/mL for the indicated time (minutes). *Top,* whole cell extracts were prepared and resolved by SDS-PAGE, and Western blotting was done with antibodies against HIF-1α and α-tubulin. *Bottom,* quantification of the HIF-1α signal by densitometry following normalization to actin levels. HIF-1α levels from each cell at time zero are arbitrarily given the value of 1. *C,* PC-3-Neo and PC-3-MSF-A cells were labeled with [^{35}S]methionine and pulse chased in complete medium for the indicated time (hours). *Top,* equal amounts of protein from each cell lysate were subjected to immunoprecipitation with anti-HIF-1α antibody, resolved by SDS-PAGE, and subjected to autoradiography. *Bottom,* quantification of the autoradiographic HIF-1α signal by densitometry. *D,* whole cell lysates from single clones of stably transfected PC-3 cells (expressing different amounts of Flag-MSF-A protein) grown under normoxia or hypoxia were analyzed on SDS-PAGE and immunoblotted with HIF-1α and Flag antibodies. *E,* PC-3-Neo and PC-3-MSF-A cells were treated with either 0.1% DMSO or with 5 and 20 μmol/L MG-132 for 4 hours. Whole cell lysates were prepared and equal amounts of protein from each cell lysate were resolved by SDS-PAGE, transferred, and immunoblotted with antibodies against HIF-1α and actin. Ub-HIF-1α points to ubiquinated HIF-1α protein species. *F,* PC-3-Neo and PC-3-MSF-A cells were treated with either 0.1% DMSO or with 10 μmol/L MG-132 for 4 hours. Whole cell lysates were prepared and subjected to immunoprecipitation with HIF-1α antibody. Immunoprecipitates were resolved on SDS-PAGE and immunoblotted with HIF-1α and ubiquitin antibodies. Ub-HIF-1α points to ubiquinated HIF-1α protein species.

from PC-3-Neo cells were decreased by ~50%, whereas HIF-1α protein levels in PC-3-MSF-A decreased by 50% only after 40 minutes of cycloheximide exposure (Fig. 5*B*). Although the intensity of the HIF-1α signal was different at the zero time point, the degradation rate of HIF-1α protein was faster in the PC-3-Neo cells (Fig. 5*B*). This was further confirmed when cells were labeled with [^{35}S]methionine and pulse chased, after which HIF-1α protein levels were analyzed. The half-life of HIF-1α protein from PC-3-Neo cells was around 25 minutes compared with 45 minutes in PC-3-MSF-A cells (Fig. 5*C*). Again, as shown in the graph by the slope of

the two curves in Fig. 5*B* and *C*, the rates of HIF-1α protein loss were slower in the PC-3-MSF-A cells.

When we examined the pattern of HIF-1α immunoreactive bands in different MSF-A stable clones under hypoxia (where degradation does not take place), we observed differences in the higher molecular weight bands of HIF-1α protein, which probably reflect ubiquinated and polyubiquinated HIF-1α (Ub-HIF-1α) species. The pattern of HIF-1α ubiquitination was inversely correlated with the levels of MSF-A protein expression (Fig. 5*D*). We therefore studied the ubiquitination of the endogenous HIF-1α in cells overexpressing MSF-A protein in the absence and presence of the proteasome inhibitor MG-132. Under these conditions, HIF-1α is subjected to ubiquitination but cannot be degraded through the proteasome. As shown in Fig. 5*E*, increasing doses of MG-132 induced the expression of HIF-1α and Ub-HIF-1α in the PC-3-Neo cells. On the other hand, the pattern of Ub-HIF-1α levels in the PC-3-MSF-A cells was less intense and was composed of predominantly lower molecular weight species (Fig. 5*E*). To confirm the ubiquitination forms of HIF-1α, the PC-3-Neo and PC-3-MSF-A cells were treated with MG-132 and subjected to immunoprecipitation with HIF-1α antibody. Immunoprecipitates were immunoblotted in parallel with either HIF-1α (Fig. 5*F, top*) or ubiquitin (Fig. 5*F, bottom*) antibodies. Again, the levels of the Ub-HIF-1α protein were lower in the PC-3-MSF-A cells than in the PC-3-Neo cells.

Collectively, the activation of HIF-1 by MSF-A was shown to be mediated through HIF-1α protein stabilization. MSF-A protein interacts with HIF-1α protein under normoxic conditions to modulate its ubiquitination, thus escaping proteasomal degradation.

MSF-A expression in common human tumors. To examine the expression level of MSF-A in common human cancers, we used a matched tumor/normal expression array, which includes cDNA from 68 tumors and corresponding normal tissues from individual patients. The array was hybridized with a probe that should react with all the variants of *SEPT9*, including MSF-A. The array was reprobed with β-actin control for normalization. *SEPT9* expression was quantified and analyzed for comparison between normal versus tumor specimens. As shown in Fig. 6*A*, the *SEPT9* gene was strikingly and significantly overexpressed in ovarian tumor samples compared with other tested samples. Interestingly, we also observed a lesser degree of *SEPT9* overexpression among samples of other parts of the female reproductive system, including breast and uterus (Fig. 6*A*), whereas there was almost no noticeable change in expression level in other tumor samples (Fig. 6*A*). Because the cDNA probe is not specific to the MSF-A variant, we cannot exclude a differential expression of the splice variants in the various tumors. Therefore, to extend our analysis of MSF-A expression in prostate cancer, where it was originally found to interact with HIF-1α, we did RT-PCR analysis using unique primers to specifically identify the MSF-A variant. RNA samples from various prostate cell lines and xenografts exhibited higher expression levels of MSF-A mRNA in prostate cancer samples compared with those of RNA derived from normal prostate tissue (Fig. 6*B*).

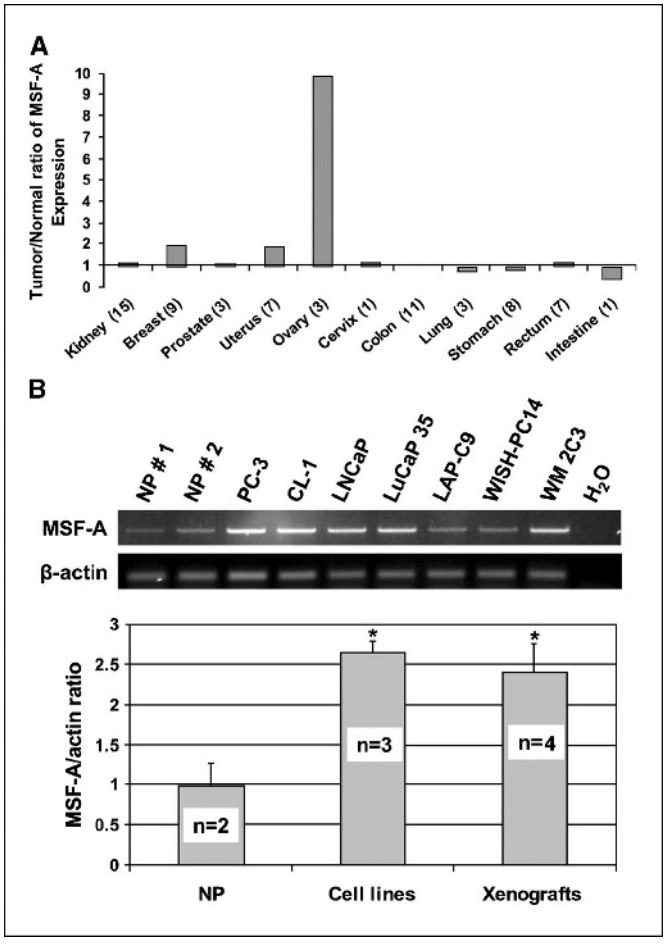

Figure 6. MSF-A mRNA expression in human tumors. *A,* a human matched tumor/normal expression array (containing 68 pairs of tumor/normal different tissues) was hybridized with probe to MSF-A (the probe also reacts with other *SEPT9* transcripts) and to β-actin. Autoradiograms were analyzed. *Columns,* expression ratio of each tumor/normal. *Numbers in parentheses,* number of pairs of each tumor type. *B, top,* total RNA was isolated from two different normal prostate tissues (*NP*), prostate cancer cell lines (PC-3, CL-1, and LNCaP), and prostate cancer xenografts (LuCaP 35, LAP-C9, WISH-PC-14, and WM 2C3), and was analyzed by RT-PCR using primers specific to MSF-A and β-actin. *Bottom,* densitometric quantification of MSF-A/actin expression in the samples tested where MSF-A/actin ratio was normalized to 1. *Column*, means; *bars*, SD. *, $P < 0.01$.

Discussion

In the present study, we identified a novel regulatory pathway by which MSF-A, a member of the mammalian septin gene family, is involved in tumorigenesis, at least in part, through the activation of the HIF-dependent response system. Our results show that MSF-A protein directly interacts with HIF-1α but not with HIF-1β (Fig. 1). Overexpression of MSF-A leads to activation of HIF-1 and up-regulation of HIF-downstream genes *in vitro* and *in vivo* (Figs. 2-4; Supplementary Fig. S2). Functionally, we show that MSF-A promotes proliferation, soft agar clonal survival, tumor growth, and vascularization (Figs. 3 and 4).

HIF-1 is a master regulator of the hypoxic response pathway, not only in physiologic processes but also in pathophysiologic states, such as ischemia and cancer (6, 32, 33). Apart from the relatively well-characterized mechanisms of hypoxic HIF-1α subunit stabilization, many growth factors and cytokines are known to stabilize HIF-1α under normoxic conditions. Despite this great diversity, most of these growth factors might stabilize HIF-1α via common cellular kinase pathways, including the

phosphoinositide-3 kinase and mitogen-activated protein kinase pathways that are activated by cell type–specific growth factors receptors (32). It is, however, not yet completely understood how HIF-1α is stabilized in cancer cells under normoxic epigenetic conditions. The importance and potential therapeutic benefits of the HIF pathway have driven the search for new regulatory components. To that end, we sought new regulators for affecting the HIF pathway. We used coimmunoprecipitation methods that revealed an interaction between MSF-A and HIF-1α (Fig. 1).

MSF-A is a splice variant of the *SEPT9* of the mammalian septin gene family (34): It was first found as a fusion partner gene of *MLL* in a case of therapy-related acute myeloid leukemia with a t(11, 17)(q23;q25) translocation (22, 35). Septins were originally discovered in yeast and found to be involved in diverse cellular processes, including cytokinesis, vesicle trafficking, apoptosis, and maintenance of cell polarity (24). The family of human septins shows considerable homology in the core GTP-binding domain but divergence in the NH_2 and COOH termini (23, 24). Whereas most of the available data on the biology of septins are derived from yeast, little is known about the physiologic and the pathophysiologic significance of septins in mammals. Several lines of evidence suggest a role for septins in oncogenesis. Some of septin genes (e.g., *SEPT5, SEPT6, SEPT9*, and *SEPT11*) are involved in chromosomal translocations in myeloid leukemias with the formation of chimeric MLL fusion proteins (24). *SEPT9* was recently found to be altered in human ovarian cancer (36), consistent with our ovarian cancer results (Fig. 6*A*), and was shown to be amplified and overexpressed in breast cancer (37). In addition, Scott et al. (25) reported very recently a meticulous analysis of *SEPT9* RNA expression in a wide range of human tumors and found that *SEPT9* is overexpressed in breast, central nervous system, endometrium, kidney, liver, lung, lymphoid, esophagus, ovary, pancreas, skin, soft tissue, and thyroid cancers. In the current study, we found that MSF-A is specifically up-regulated in prostate cancer cell lines and xenografts as well (Fig. 6*B*). Interestingly, HIF-1α overexpression is also observed in the majority of human cancers (38). The mechanisms of HIF-1α overexpression in most cancers are not yet known where VHL is not mutated. Our data support the hypothesis that some human cancers have HIF-1α activated by septins independent of hypoxia.

MSF-A expression augments the activity of HIF-1 and induces higher proliferation rates both under normoxia and hypoxia as well as *in vitro* and *in vivo* (Figs. 2 and 3). However, it should be kept in mind that the effects of MSF-A on proliferation could not be only attributed to HIF activation but also to other yet unknown effects of MSF-A protein independent of HIF pathway. Furthermore, MSF-A affects the pattern of tumor necrosis with overall increased vascularity within tumors (Fig. 3). The current study provides the first observation that a septin protein has effects on tumor angiogenesis.

A number of septins have been shown to bind and hydrolyze guanine nucleotide but the role of GTP binding and hydrolysis in septin function has not been fully elucidated (39–43). In our study, deletion of the GTP-binding domain in MSF-A abolished its effects on HIF-1 transcriptional activity (Fig. 1), whereas the mutant lacking the GTP-binding site still retained ability to interact with HIF-1α protein. On the other hand, deletion of the unique NH_2-terminal domain of MSF-A, which contains nuclear target sequence, exhibited a dominant negative effect on HIF transcriptional activity (Fig. 1). Our results indicate that induction of HIF transcriptional activity by MSF-A is dependent on these critical domains and that the activation requires binding and/or hydrolysis of GTP. It has been shown previously that Rac1 of the small GTPase Rho family is activated in response to hypoxia and is required for the induction of HIF-1α protein expression and transcriptional activity in hypoxic cells (44). Very recently, Nagata and Inagaki (45) identified a Rho-guanine nucleotide exchange factor as a binding partner for MSF-A, describing the first link between septins and Rho signaling. It is reasonable to speculate that the activation of HIF-1 by Rho could be mediated through interactions involving MSF-A.

Mechanistically, our data show that MSF-A affects HIF-1α protein at the posttranslational level (Fig. 5). HIF-1α protein interacts preferentially with MSF-A protein under normoxia similar to VHL. This interaction reduces HIF-1α ubiquitination and decreases its degradation rate resulting in HIF-1α stabilization as shown by the protein stability studies done under normoxia (Fig. 5). Although this stabilization is not sufficient to affect the steady-state levels of HIF-1α protein, it becomes rate limiting during hypoxia. One possible explanation is that MSF-A effects on HIF-1 activation is attributed to the stabilizing effects under normoxia by leaving a higher number of HIF-1α molecules available for activation under hypoxia. Of course, it should be taken into account that there could be other possible mechanisms for HIF-1 activation by MSF-A independent of MSF-A/HIF-1α direct interaction. It is also not yet clear whether MSF-A inhibits HIF-1α ubiquitination by preventing its proline hydroxylation or by modulating VHL E3-ligase activity. Further studies are necessary to elucidate the exact mechanism by which MSF-A stabilizes HIF-1α.

To further confirm the link between HIF-1α and MSF-A, we sought small interfering RNA sequences to exclusively knock down MSF-A. Unfortunately, because of the high degree of homology of the various *SEPT9* transcripts, we could not identify small interfering RNA sequences from the limited number of candidates to knock down only MSF-A but not other variants of *SEPT9* (data not shown).

The interactions between HIF-1α and MSF-A, in addition to their colocalization, and the functional activation of HIF-1 by MSF-A may represent a role of *SEPT9* function in tumorigenesis. Further studies are essential for understanding the physiologic and pathophysiologic significance of septin-HIF regulation in human cancers.

Acknowledgments

Received 8/3/2005; revised 10/15/2005; accepted 10/26/2005.

Grant support: M.K. Humanitarian Association and PCF Israel, Avon Breast Cancer Foundation, Department of Defense Manhattan Project for Prostate Cancer Research, Bat Sheva De Rothschild Foundation, and Israel Cancer Association.

The costs of publication of this article were defrayed in part by the payment of page charges. This article must therefore be hereby marked *advertisement* in accordance with 18 U.S.C. Section 1734 solely to indicate this fact.

We thank Esther Eshkol for editorial assistance, and Dr. Letizia Schreiber-Bramante (Department of Pathology, Tel Aviv Sourasky Medical Center, Tel Aviv, Israel) and Prof. Ilan Hammel (Department of Pathology, Sackler Faculty of Medicine, Tel Aviv University, Tel Aviv, Israel) for helping in analyzing and quantifying immunohistochemical staining; Prof. Yosef Yarden and Dr. Sara Lavie for helping with the animal experiments (Department of Biological Regulation, Weizmann Institute of Science, Rehovot, Israel); Prof. Zelig Eshhar (Department of Immunology, Weizmann Institute of Science, Rehovot, Israel) for providing prostate cancer RNA samples; and Prof. Avi Orr-Urtreger and Drs. Anat Bar-Shira and Helena Yagev-More (Department of Genetics, Tel Aviv Sourasky Medical Center, Tel Aviv, Israel) for helping in performing real-time PCR reactions.

References

1. Melillo G. HIF-1: a target for cancer, ischemia and inflammation—too good to be true? Cell Cycle 2004;3:154–5.
2. Bardos JI, Ashcroft M. Hypoxia-inducible factor-1 and oncogenic signalling. Bioessays 2004;26:262–9.
3. Hopfl G, Ogunshola O, Gassmann M. HIFs and tumors—causes and consequences. Am J Physiol Regul Integr Comp Physiol 2004;286:R608–23.
4. Semenza GL. Hydroxylation of HIF-1: oxygen sensing at the molecular level. Physiology 2004;19:176–82.
5. Vaupel P. The role of hypoxia-induced factors in tumor progression. Oncologist 2004;9 Suppl 5:10–7.
6. Semenza GL. Targeting HIF-1 for cancer therapy. Nat Rev Cancer 2003;3:721–32.
7. Bruick RK, McKnight SL. A conserved family of prolyl-4-hydroxylases that modify HIF. Science 2001;294:1337–40.
8. Metzen E, Berchner-Pfannschmidt U, Stengel P, et al. Intracellular localisation of human HIF-1α hydroxylases: implications for oxygen sensing. J Cell Sci 2003;116:1319–26.
9. Epstein AC, Gleadle JM, McNeill LA, et al. C. elegans EGL-9 and mammalian homologs define a family of dioxygenases that regulate HIF by prolyl hydroxylation. Cell 2001;107:43–54.
10. Ivan M, Kondo K, Yang H, et al. HIFα targeted for VHL-mediated destruction by proline hydroxylation: implications for O_2 sensing. Science 2001;292:464–8.
11. Mahon PC, Hirota K, Semenza GL. FIH-1: a novel protein that interacts with HIF-1α and VHL to mediate repression of HIF-1 transcriptional activity. Genes Dev 2001;15:2675–86.
12. Hewitson KS, McNeill LA, Riordan MV, et al. Hypoxia-inducible factor (HIF) asparagine hydroxylase is identical to factor inhibiting HIF (FIH) and is related to the cupin structural family. J Biol Chem 2002;277:26351–5.
13. Lando D, Peet DJ, Gorman JJ, et al. FIH-1 is an asparaginyl hydroxylase enzyme that regulates the transcriptional activity of hypoxia-inducible factor. Genes Dev 2002;16:1466–71.
14. Quintero M, Mackenzie N, Brennan PA. Hypoxia-inducible factor 1 (HIF-1) in cancer. Eur J Surg Oncol 2004;30:465–8.
15. Brahimi-Horn MC, Pouyssegur J. The hypoxia-inducible factor and tumor progression along the angiogenic pathway. Int Rev Cytol 2005;242:157–213.
16. Kim W, Kaelin WG, Jr. The von Hippel-Lindau tumor suppressor protein: new insights into oxygen sensing and cancer. Curr Opin Genet Dev 2003;13:55–60.
17. Maxwell PH, Dachs GU, Gleadle JM, et al. Hypoxia-inducible factor-1 modulates gene expression in solid tumors and influences both angiogenesis and tumor growth. Proc Natl Acad Sci U S A 1997;94:8104–9.
18. Ryan HE, Lo J, Johnson RS. HIF-1 α is required for solid tumor formation and embryonic vascularization. EMBO J 1998;17:3005–15.
19. Ryan HE, Poloni M, McNulty W, et al. Hypoxia-inducible factor-1α is a positive factor in solid tumor growth. Cancer Res 2000;60:4010–5.
20. Carmeliet P, Dor Y, Herbert JM, et al. Role of HIF-1α in hypoxia-mediated apoptosis, cell proliferation and tumour angiogenesis. Nature 1998;394:485–90.
21. Welsh SJ, Powis G. Hypoxia inducible factor as a cancer drug target. Curr Cancer Drug Targets 2003;3:391–405.
22. Osaka M, Rowley JD, Zeleznik-Le NJ. MSF (MLL septin-like fusion), a fusion partner gene of MLL, in a therapy-related acute myeloid leukemia with a t(11;17)(q23;q25). Proc Natl Acad Sci U S A 1999;96:6428–33.
23. Kartmann B, Roth D. Novel roles for mammalian septins: from vesicle trafficking to oncogenesis. J Cell Sci 2001;114:839–44.
24. Hall PA, Russell SE. The pathobiology of the septin gene family. J Pathol 2004;204:489–505.
25. Scott M, Hyland PL, McGregor G, et al. Multimodality expression profiling shows SEPT9 to be overexpressed in a wide range of human tumours. Oncogene 2005;24:4688–700.
26. Hall PA, Jung K, Hillan KJ, Russell SH. Expression profiling the human septin gene family. J Pathol 2005;206:269–78.
27. Mabjeesh NJ, Post DE, Willard MT, et al. Geldanamycin induces degradation of hypoxia-inducible factor 1α protein via the proteosome pathway in prostate cancer cells. Cancer Res 2002;62:2478–82.
28. Mabjeesh NJ, Escuin D, LaVallee TM, et al. 2ME2 inhibits tumor growth and angiogenesis by disrupting microtubules and dysregulating HIF. Cancer Cell 2003;3:363–75.
29. Post DE, Van Meir EG. Generation of bidirectional hypoxia/HIF-responsive expression vectors to target gene expression to hypoxic cells. Gene Ther 2001;8:1801–7.
30. David A, Mabjeesh N, Azar I, et al. Unusual alternative splicing within the human kallikrein genes KLK2 and KLK3 gives rise to novel prostate-specific proteins. J Biol Chem 2002;277:18084–90.
31. Zhong H, Agani F, Baccala AA, et al. Increased expression of hypoxia inducible factor-1α in rat and human prostate cancer. Cancer Res 1998;58:5280–4.
32. Wenger RH. Cellular adaptation to hypoxia: O_2-sensing protein hydroxylases, hypoxia-inducible transcription factors, and O_2-regulated gene expression. FASEB J 2002;16:1151–62.
33. Maxwell PH, Ratcliffe PJ. Oxygen sensors and angiogenesis. Semin Cell Dev Biol 2002;13:29–37.
34. Macara IG, Baldarelli R, Field CM, et al. Mammalian septins nomenclature. Mol Biol Cell 2002;13:4111–3.
35. Taki T, Ohnishi H, Shinohara K, et al. AF17q25, a putative septin family gene, fuses the MLL gene in acute myeloid leukemia with t(11;17)(q23;q25). Cancer Res 1999;59:4261–5.
36. Burrows JF, Chanduloy S, McIlhatton MA, et al. Altered expression of the septin gene, SEPT9, in ovarian neoplasia. J Pathol 2003;201:581–8.
37. Montagna C, Lyu MS, Hunter K, et al. The Septin 9 (MSF) gene is amplified and overexpressed in mouse mammary gland adenocarcinomas and human breast cancer cell lines. Cancer Res 2003;63:2179–87.
38. Zhong H, De Marzo AM, Laughner E, et al. Overexpression of hypoxia-inducible factor 1α in common human cancers and their metastases. Cancer Res 1999;59:5830–5.
39. Field CM, al-Awar O, Rosenblatt J, et al. A purified *Drosophila* septin complex forms filaments and exhibits GTPase activity. J Cell Biol 1996;133:605–16.
40. Gladfelter AS, Bose I, Zyla TR, Bardes ES, Lew DJ. Septin ring assembly involves cycles of GTP loading and hydrolysis by Cdc42p. J Cell Biol 2002;156:315–26.
41. Mendoza M, Hyman AA, Glotzer M. GTP binding induces filament assembly of a recombinant septin. Curr Biol 2002;12:1858–63.
42. Versele M, Thorner J. Septin collar formation in budding yeast requires GTP binding and direct phosphorylation by the PAK, Cla4. J Cell Biol 2004;164:701–15.
43. Robertson C, Church SW, Nagar HA, et al. Properties of SEPT9 isoforms and the requirement for GTP binding. J Pathol 2004;203:519–27.
44. Hirota K, Semenza GL. Rac1 activity is required for the activation of hypoxia-inducible factor 1. J Biol Chem 2001;276:21166–72.
45. Nagata K, Inagaki M. Cytoskeletal modification of Rho guanine nucleotide exchange factor activity: identification of a Rho guanine nucleotide exchange factor as a binding partner for Sept9b, a mammalian septin. Oncogene 2005;24:65–76.